

# Hyperfine interactions in $\text{Tb}_{0.27}\text{Dy}_{0.73}(\text{Fe}_{1-x}\text{Co}_x)_2$ compounds at 77 K

Wiktor Bodnar,  
Monika Szklarska-Łukasik,  
Paweł Stoch,  
Piotr Zachariasz,  
Jarosław Pszczoła,  
Jan Suwalski

**Abstract.** The synthesis of materials, crystal structure and  $^{57}\text{Fe}$  Mössbauer effect studies at 77 K were performed for intermetallics  $\text{Tb}_{0.27}\text{Dy}_{0.73}(\text{Fe}_{1-x}\text{Co}_x)_2$ . The starting compound  $\text{Tb}_{0.27}\text{Dy}_{0.73}\text{Fe}_2$  of this Fe/Co substituted series is known as Terfenol-D. XRD measurements evidence a pure cubic Laves phase C15,  $\text{MgCu}_2$ -type. The determined unit cell parameter decreases across the series. Co substitution introduces a local area, in the subnanoscale, with random Fe/Co neighbourhoods of the  $^{57}\text{Fe}$  atoms. Mössbauer effect spectra for the  $\text{Tb}_{0.27}\text{Dy}_{0.73}(\text{Fe}_{1-x}\text{Co}_x)_2$  series collected at 77 K consist of a number of locally originated subspectra due to random composition of Fe and Co atoms in the nearest neighbourhood. Hyperfine interaction parameters: isomer shift, magnetic hyperfine field and a quadrupole interaction parameter were obtained from the fitting procedure of the spectra, both for the local area and for the sample as bulk. As a result of Fe/Co substitution, a Slater-Pauling type curve for the average magnetic hyperfine field vs. Co content in the  $\text{Tb}_{0.27}\text{Dy}_{0.73}(\text{Fe}_{1-x}\text{Co}_x)_2$  series is observed. It is found that the magnetic hyperfine fields corresponding to the local area sorted out against Co contribution in the Fe/Co neighbourhoods also create a dependence similar to the Slater-Pauling type curve.

**Key words:** intermetallics • crystal structure • Laves phase • Mössbauer effect • hyperfine interaction • Slater-Pauling dependence

W. Bodnar, M. Szklarska-Łukasik, J. Pszczoła<sup>✉</sup>  
Faculty of Physics and Applied Computer Science,  
AGH University of Science and Technology,  
30 A. Mickiewicza Ave., 30-059 Kraków, Poland,  
Tel.: +48 12 617 2990, Fax: +48 12 634 0010,  
E-mail: pszczola@agh.edu.pl

P. Stoch  
Institute of Atomic Energy,  
05-400 Otwock-Świerk, Poland  
and Faculty of Material Science and Ceramics,  
AGH University of Science and Technology,  
30 A. Mickiewicza Ave., 30-059 Kraków, Poland

P. Zachariasz, J. Suwalski  
Institute of Atomic Energy,  
05-400 Otwock-Świerk, Poland

Received: 21 September 2009  
Accepted: 17 November 2009

## Introduction

Heavy rare earth (*R*) – transition metal (*M*) compounds with formula  $RM_2$  have been widely studied for scientific and practical reasons [2–4, 28]. The ferrimagnetism of these intermetallics depends on both the rare earth constituent ( $4f5d$  electrons) and the transition metal constituent ( $3d$  electrons) [5].

For instance, the significance of the  $3d$  electrons has been previously experimentally studied in the  $\text{Dy}(\text{Fe}_{1-x}\text{Co}_x)_2$  intermetallics series using the  $^{57}\text{Fe}$  Mössbauer effect [11, 12, 26]. The magnetic hyperfine field  $\mu_0 H_{\text{hf}}$  ( $\mu_0$  is the magnetic permeability) observed at  $^{57}\text{Fe}$  nuclei treated as a function of the average number  $n$  of  $3d$  electrons behaves according to the Slater-Pauling curve [11, 12, 26].

Additionally, it has been found that the Curie temperature  $T_C(n)$ , as a result of Fe/Co substitution, also changes resembling the Slater-Pauling curve to some extent.

From the practical point of view,  $R\text{Fe}_2$  type materials have been previously studied because of their strong magnetostriction [6, 7, 30]. In order to find material with high magnetostriction the Tb/Dy substitution in the rare earth sublattice has been applied. Namely, the series of materials  $\text{Tb}_x\text{Dy}_{1-x}\text{Fe}_2$  has been studied and

especially strong magnetostriction has been derived in the  $\text{Tb}_{0.27}\text{Dy}_{0.73}\text{Fe}_2$  compound, often called Terfenol-D [6, 7, 30].

Recently, both Terfenol-D and other intermetallics of the series  $\text{Tb}_x\text{Dy}_{1-x}\text{Fe}_2$  have been widely used as strongly magnetostrictive constituents of composites with piezoceramics in order to obtain materials with a giant magnetoelectric effect [10, 18, 19, 31].

Fe/Co substitution in  $R\text{Fe}_2$  type compounds changes the number  $n$  of  $3d$  electrons in the  $M$  sublattice, strongly influencing the  $3d$ -band and thus the magnetism, and the hyperfine interactions. It was, therefore, interesting to study the influence of the  $3d$ -band electron population on the magnetism of the  $3d$ -sublattice and especially on the hyperfine interaction parameters in Terfenol-D type compounds with Co substitution. Specifically, it was interesting to study systematically by the Mössbauer effect the  $\text{Tb}_{0.27}\text{Dy}_{0.73}(\text{Fe}_{1-x}\text{Co}_x)_2$  intermetallics with Terfenol-D as the starting compound of this Fe/Co substituted series, which can be treated as potential constituents of composite and laminate magnetoelectric materials [10, 18, 19, 31].

## Materials and X-ray studies

Polycrystalline intermetallics  $\text{Tb}_{0.27}\text{Dy}_{0.73}(\text{Fe}_{1-x}\text{Co}_x)_2$  ( $x = 0, 0.1, \dots, 0.9$  and  $1.0$ ) were synthesized by arc melting with contact-less ignition in a high purity argon atmosphere using appropriate amounts of Tb (99.9%), Dy (99.9%), Fe and Co (99.99% purity) [25]. For the sake of homogenization, the obtained ingots were annealed in vacuum at 1200 K for 12 h and then cooled down along with the furnace (cooling: approximately 250 K/h).

The post-annealed compounds were micromilled and their phase homogeneity and crystal structure were studied with standard X-ray powder diffraction measurements (XRD) using  $\text{MoK}\alpha$  radiation. The X-ray patterns obtained for these compounds were analyzed using a Rietveld-type procedure adopting both the  $\text{K}\alpha_1$  (wavelength  $\lambda_1 = 0.70930 \text{ \AA}$ ) and  $\text{K}\alpha_2$  (wavelength  $\lambda_2 = 0.71359 \text{ \AA}$ ) lines [21, 22]. A clean cubic,  $Fd\bar{3}m$ ,  $\text{MgCu}_2$ -type, C15 crystal structure was observed for all the studied compounds. The C15-Laves phase crystal structure has been described in detail elsewhere [17].

It can be added that in the C15 crystal structure each transition metal atom is surrounded by six transition metal atoms as nearest neighbours [17].

Since the atomic radius of Fe ( $r_{\text{Fe}} = 1.72 \text{ \AA}$ ) is larger as compared to the corresponding radius of Co ( $r_{\text{Co}} = 1.67 \text{ \AA}$ ), the unit cell parameter described by the following numerical formula:  $a(x) = (-0.104x^2 - 0.029x + 7.337) \text{ \AA}$  decreases softly non-linearly with cobalt content  $x$  (Fig. 1, curve 1) [27]. This formula is used to follow the experimental points and is obtained by a least squares fitting procedure. The values of the studied series coincide satisfactorily with the existing fragmentary literature data (open points in Fig. 1) [8, 13–15, 20, 32]. The unit cell volume is described by the following numerical formula:  $V(x) = (-17.143x^2 - 4.295x + 394.950) \text{ \AA}^3$  and it decreases softly non-linearly like the lattice parameter with increasing cobalt content  $x$  (Fig. 1, curve 2). The convex deviation  $a(x)$  and  $V(x)$

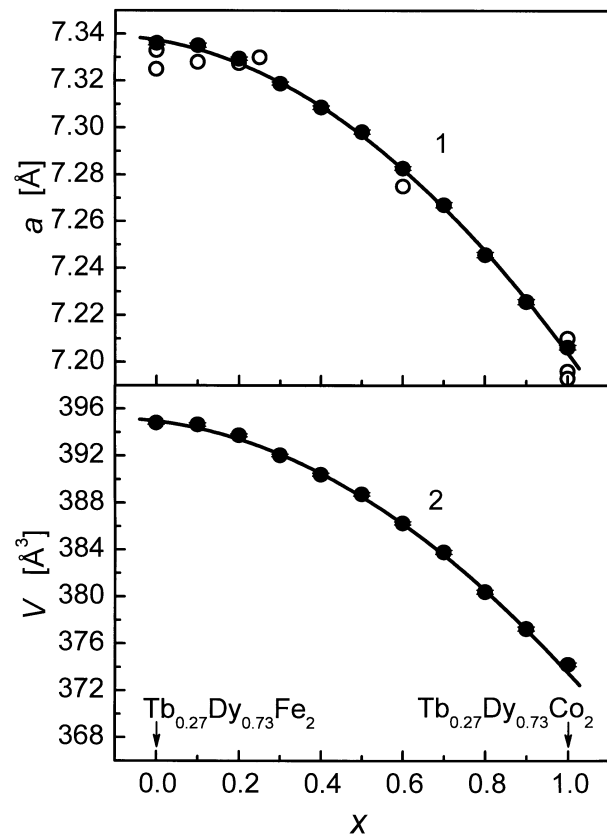


**Fig. 1.** The unit cell parameters (curve 1) and the unit cell volumes (curve 2) of the  $\text{Tb}_{0.27}\text{Dy}_{0.73}(\text{Fe}_{1-x}\text{Co}_x)_2$  intermetallic system (300 K). Open points taken from literature [8, 13–15, 20, 32].

from Vegard's rule, i.e. from linear dependence, is observed as being typical of  $R$ - $M$  intermetallics. It is expected that presumably a magnetovolume effect introduces this convex deviation.

## $^{57}\text{Fe}$ Mössbauer effect

### Spectra and analysis

The  $^{57}\text{Fe}$  Mössbauer patterns, presented in Fig. 2, were collected at 77 K by using a standard transmission technique with a  $^{57}\text{Co}$  source in Pd. Spectra characteristic of the [100] easy axis of magnetization were fitted, assuming the random distribution of the Fe/Co atoms in the transition metal sublattice.

The random distribution of the Fe/Co atoms in the transition metal sublattice introduces different neighbourhoods of the probed iron atom; it can be surrounded by  $(6-k)$  iron atoms and  $k$  cobalt atoms ( $k = 0, 1, 2, \dots, 6$ ) as nearest neighbours. Particularly Fe/Co surrounding determines locally its own subspectrum contributing to the resulting measured Mössbauer effect pattern and, therefore, introducing its proper hyperfine interaction parameters. The probability of particular neighbourhoods and thus subspectra  $P(6;k) = \{[6! / (6-k)!k!] \cdot (1-x)^{6-k} x^k\}$  is described by the Bernoulli distribution, in this case adapted for the intermetallic formula  $\text{Tb}_{0.27}\text{Dy}_{0.73}(\text{Fe}_{1-x}\text{Co}_x)_2$  [9]. During the fitting procedure, it was assumed that intensities  $A(k)$  of particular subspectra follow the probabilities  $P(6;k)$ .

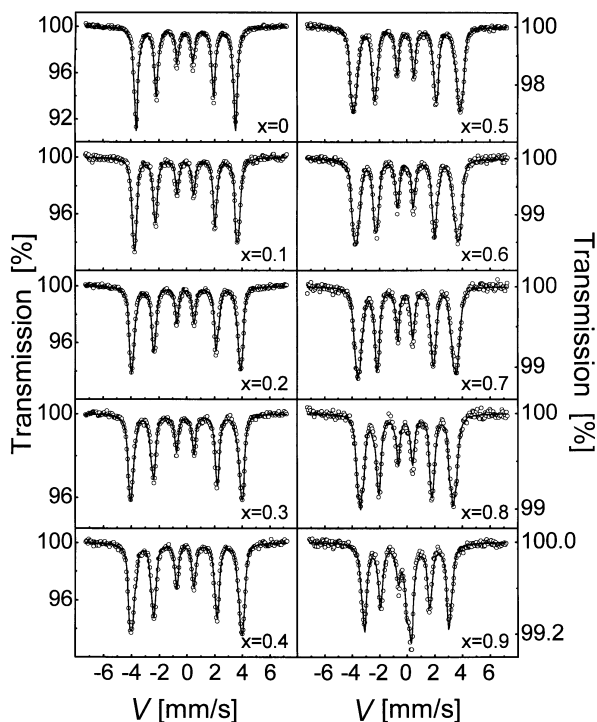


**Fig. 2.**  $^{57}\text{Fe}$  Mössbauer effect transmission spectra of the  $\text{Tb}_{0.27}\text{Dy}_{0.73}(\text{Fe}_{1-x}\text{Co}_x)_2$  intermetallics (77 K).

Surroundings with probabilities less than 0.1 of maximal probability were not considered. For this reason, the remaining considered probabilities were normalized again.

### Local hyperfine magnetic fields

The magnetic hyperfine fields,  $\mu_0 H_{\text{hf}}$ , corresponding to particular subspectra of the series  $\text{Tb}_{0.27}\text{Dy}_{0.73}(\text{Fe}_{1-x}\text{Co}_x)_2$  determined from the fitting procedure treated as functions of number  $k$  are presented in Fig. 3. The individual dependencies,  $\mu_0 H_{\text{hf}}$ , against  $k$ , obtained for particular compounds and, therefore, labelled with the  $x$ -parameter, are presented in the figure. Additionally, Fig. 3 (dashed lines 1 and 2) shows the arithmetically averaged magnetic hyperfine fields,  $\mu_0 H_{\text{hf}}$ , against the number  $k$  of Co atoms in the nearest

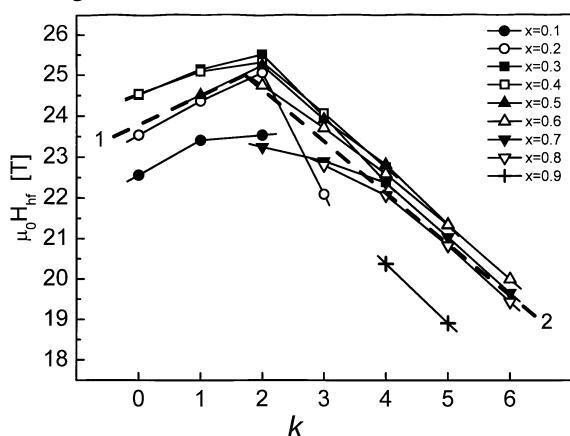


**Fig. 3.** The fitted magnetic hyperfine field  $\mu_0 H_{\text{hf}}$  labelled with  $x$  as function of  $k$  for the  $\text{Tb}_{0.27}\text{Dy}_{0.73}(\text{Fe}_{1-x}\text{Co}_x)_2$  series; averaged values – dashed lines 1 and 2.

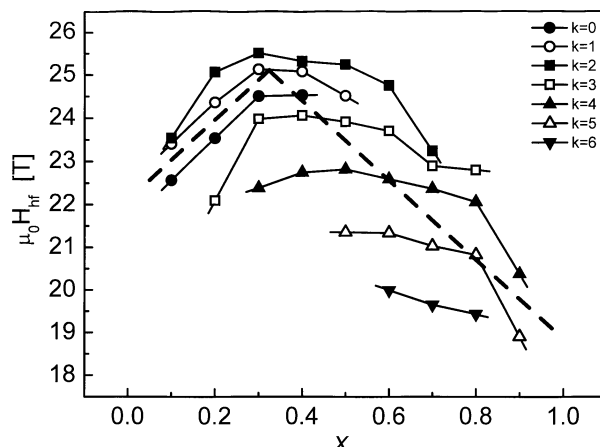


**Fig. 4.** The  $\mu_0 H_{\text{hf}}$  magnetic hyperfine fields vs.  $x$  of the  $\text{Tb}_{0.27}\text{Dy}_{0.73}(\text{Fe}_{1-x}\text{Co}_x)_2$  series determined at different  $k$  values. The average values – dashed line.

neighbourhood. It can be noticed that both the individual dependencies and the average dependence as a function of  $k$  resemble the Slater-Pauling curve. Dashed lines 1 and 2 in Fig. 3 are described by the numerical formulae  $\mu_0 H_{\text{hf}}(k) = (0.71k + 23.79)\text{T}$  and  $\mu_0 H_{\text{hf}}(k) = (-1.27k + 27.18)\text{T}$ , correspondingly.

It is interesting to present the fitted particular, or locally originated, magnetic hyperfine field data again in Fig. 4. In this case the dependencies of the local  $\mu_0 H_{\text{hf}}$  fields, ascribed to the corresponding  $k$  values, treated as functions of the composition parameter  $x$ , i.e. determined for different compounds, are presented in the figure. The dashed line presents the average of the magnetic hyperfine fields calculated using the Bernoulli distribution formula [9].

### Average hyperfine interaction parameters

The average hyperfine interaction parameters weighted by the subspectra intensities, which follow the Bernoulli distribution, i.e. the isomer shift IS (with respect to iron metal, at 300 K), the magnetic hyperfine field  $\mu_0 H_{\text{hf}}$  and the quadrupole interaction parameter QS [29], determined across the  $\text{Tb}_{0.27}\text{Dy}_{0.73}(\text{Fe}_{1-x}\text{Co}_x)_2$  series at 77 K, are presented in Fig. 5.

The isomer shift IS is described by the numerical formula  $\text{IS}(x) = (-0.130x^2 + 0.098x + 0.025)$  mm/s (Fig. 5, line 1). For  $x = 0$  almost the same value of IS has been obtained elsewhere [24].

The average  $\mu_0 H_{\text{hf}}$  dependence is presented as two sections described by the numerical formulae:  $\mu_0 H_{\text{hf}}(x) = (9.30x + 22.11)\text{T}$  (Fig. 5, line 2.1) and  $\mu_0 H_{\text{hf}}(x) = (-9.26x + 28.11)\text{T}$  (Fig. 5, line 2.2). Figure 5 also contains fragmentary literature data [23, 24].

The experimental pattern for  $x = 0.9$  has been fitted considering also the subspectrum corresponding to the non-magnetic surrounding ( $k = 6$ ) with the zero magnetic hyperfine field. Black points in Fig. 5 presented for  $x = 0.9$  are the average values corresponding to the magnetic surroundings, whereas the open points present the average values calculated considering also the non-magnetic case.

A Slater-Pauling type dependence is observed for the average magnetic hyperfine field. At first, a weak

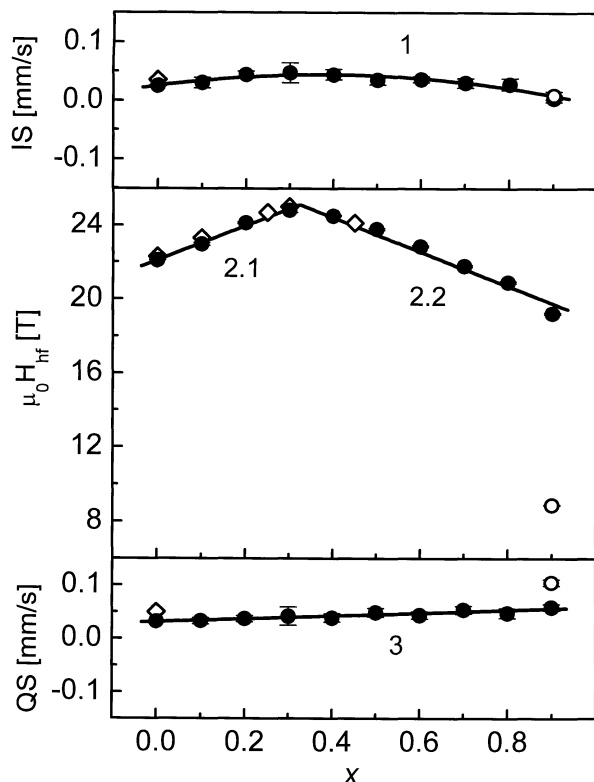


**Fig. 5.** Hyperfine interaction parameters: the isomer shift IS (line 1), the magnetic hyperfine field  $\mu_0 H_{\text{hf}}$  (lines 2.1 and 2.2) and the quadrupole interaction parameter QS (line 3) of the  $\text{Tb}_{0.27}\text{Dy}_{0.73}(\text{Fe}_{1-x}\text{Co}_x)_2$  series. Rhomboids denote literature data [16, 23, 24].

ferromagnetic type behaviour of the  $M$ -sublattice appears. This means that two  $3d$  subbands with opposite spin are not filled up [1]. The magnetic hyperfine field across the  $\text{Tb}_{0.27}\text{Dy}_{0.73}(\text{Fe}_{1-x}\text{Co}_x)_2$  series grows with  $x$  and the maximum value of the field is approached at  $x = 0.3$ . At this composition, the filling up of the majority  $3d$  subband by  $3d$  electrons is terminated.

At higher Co-substitution, a strong ferromagnetic type behaviour of the  $M$ -sublattice is observed [1]. The filling up of the minority  $3d$  subband still proceeds and the observed field decreases gradually with  $x$ . Since for the  $\text{Tb}_{0.27}\text{Dy}_{0.73}(\text{Fe}_{1-x}\text{Co}_x)_2$  compounds mostly Curie temperatures are relatively high, it is expected that magnetic moments at 77 K are not specially distanced from their magnetic saturation [8, 15, 20, 24].

The quadrupole parameter QS changes slightly with  $x$  and can be described by the numerical formula:  $\text{QS}(x) = (0.027x + 0.031)$  mm/s (Fig. 5, line 3). The parameter QS for  $x = 0$  fits well to the literature value [16].

The determined hyperfine interaction parameters coincide satisfactorily with those fragmentary data already known in the literature [16, 23, 24].

#### Correlation between magnetic fields

A comparison of the average local magnetic hyperfine field  $\mu_0 H_{\text{hf}}$  as a function of  $k$ , (Fig. 3) and  $\mu_0 H_{\text{hf}}$  as a function of  $x$ , the bulk type average magnetic hyperfine field (function of  $x$ , Fig. 5) is the subject of interest. Namely, in Fig. 6 the correlation between  $\mu_0 H_{\text{hf}}(k)$  and

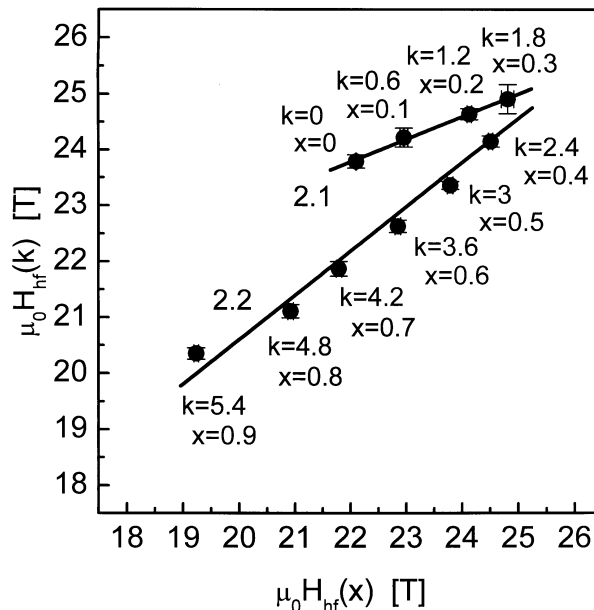


**Fig. 6.** Correlations between magnetic hyperfine fields  $\mu_0 H_{\text{hf}}(k)$  and  $\mu_0 H_{\text{hf}}(x)$ . Sections 2.1 and 2.2 correspond to those in Fig. 5. Points described by  $x$  and  $k$  values.

$\mu_0 H_{\text{hf}}(k)$  is given. The points in the figure are marked by the numbers  $x$  and  $k$ .

The  $k$ -values, a sort of local composition parameters in the nearest neighbourhood used for presentation of Fig. 6, are calculated using the proportion rule  $x:1 = k:6$  where, as mentioned previously, six denotes the number of the nearest neighbours surrounding the studied Fe atom, and  $k$  is the average number of Co atoms (not necessarily an integral number) in the neighbourhood [4, 17, 28]. The used  $k$ -value imitates locally the bulk composition parameter  $x$  of the  $\text{Tb}_{0.27}\text{Dy}_{0.73}(\text{Fe}_{1-x}\text{Co}_x)_2$  series.

The  $\mu_0 H_{\text{hf}}(k)$  dependence correlated with  $\mu_0 H_{\text{hf}}(x)$  dependence can be divided into two sections 2.1 and 2.2 (sections numbered as in Fig. 5) described by the numerical formulae:  $\mu_0 H_{\text{hf}}(k) = (0.41 \mu_0 H_{\text{hf}}(x) + 14.86)$  T (Fig. 6, line 2.1) and  $\mu_0 H_{\text{hf}}(k) = (0.79 \mu_0 H_{\text{hf}}(x) + 4.77)$  T (Fig. 6, line 2.2), correspondingly.

Considering Figs. 3 and 5, it can be seen that, section by section, a linear correlation between  $\mu_0 H_{\text{hf}}(k)$  and  $\mu_0 H_{\text{hf}}(x)$ -values appears (Fig. 6). As mentioned above, section 2.1 corresponds to what may be called the weak ferromagnetism, whereas section 2.2 corresponds to strong ferromagnetism of the transition metal sublattice.

#### Summary

Co-substitution in the  $\text{Tb}_{0.27}\text{Dy}_{0.73}(\text{Fe}_{1-x}\text{Co}_x)_2$  series introduces a number of essential changes. First of all, it introduces an additional  $3d$  electron per atom into the transition metal sublattice. Next, it decreases the lattice parameter and the unit cell volume with  $x$ , and thus decreases the average distance between the nearest neighbour  $3d$ -atoms. These changes strongly influence the band structure, especially the  $3d$  band structure and, in consequence, all the observed physical properties, including hyperfine interactions observed at iron nuclei.

Here, it is interesting to summarize the following aspect of Co-substitution. Namely, Co-substitution leads to differences in the local neighbourhoods of the probed iron atoms. Consequently, the local character of the magnetic hyperfine field is demonstrated, each Fe/Co neighbourhood of the probed Fe atom introduces its own local  $\mu_0 H_{\text{hf}}$  dependence as a function of  $x$ , resembling the Slater-Pauling curve (Fig. 4). Moreover, the magnetic hyperfine fields  $\mu_0 H_{\text{hf}}$  corresponding to the different Fe/Co neighbourhoods also create local type Slater-Pauling dependencies against the number  $k$  (Fig. 3). Thus, considering the above data and the fact that the magnetic hyperfine field approximately scales the magnetic moment, the local character of the  $3d$ -magnetic moment and consequently of the  $3d$ -band in these intermetallics can be deduced.

As a result of Fe/Co substitution, the average value of magnetic hyperfine field  $\mu_0 H_{\text{hf}}$  treated as a function of the composition parameter  $x$ , calculated for the sample as bulk, creates a Slater-Pauling dependence (Fig. 5).

It is interesting to see that the correlation between the average value of  $\mu_0 H_{\text{hf}}(k)$  (taken from Fig. 3) and the average value of  $\mu_0 H_{\text{hf}}(x)$  (taken from Fig. 5) constitute, section by section, linear dependencies, as presented in Fig. 6. These correlations also suggest that the locally originated magnetic hyperfine fields ascribed to the sub-nanoscale area distribute following a Slater-Pauling dependence.

Both the magnetic fields, average  $\mu_0 H_{\text{hf}}$  as a function of  $x$  and  $\mu_0 H_{\text{hf}}$  as a function of  $k$ , correspond to weak ferromagnetism for  $x \leq 0.3$  and  $k \leq 2$ , and to strong ferromagnetism for  $x > 0.3$  and  $k > 2$  in the transition metal sublattice. This result can be helpful both in band type calculations and for practical applications of the Terfenol-D type  $\text{Tb}_{0.27}\text{Dy}_{0.73}(\text{Fe}_{1-x}\text{Co}_x)_2$  compounds, which can be potentially treated as particulate constituents of the magnetoelectric composites.

**Acknowledgment.** Supported partially by the Polish Ministry of Science and Higher Education, project no. R015000504 and partially by AGH, projects no. 10.10.220.476 and 11.11.220.01.

## References

- Barbara B, Gignoux D, Vettier C (1988) Lectures on modern magnetism. Science Press Beijing, Berlin Heidelberg
- Burzo E, Chełkowski A, Kirchmayr HR, Madelung O, Wijn HPJ (eds) (1990) Landolt-Börnstein numerical data and functional relationships in science and technology. New Series, Group III. Vol. 19, subvol. d2. Springer, Berlin
- Burzo E, Kirchmayr HR, Gschneidner KA Jr, Eyring L (eds) (1989) Handbook on the physics and chemistry of rare earths. Vol. 12. North-Holland Publ. Co, Amsterdam
- Buschow KHJ (1980) Rare earth compounds. In: Wohlfarth EP (ed) (1980) Ferromagnetic materials. Vol. 1. North-Holland Publ. Co, Amsterdam, pp 297–414
- Campbell IA (1972) Indirect exchange for rare earths in metals. J Phys F: Met Phys 2:L47–L50
- Clark AE (1980) Magnetostrictive rare earth-Fe<sub>2</sub> compounds. In: Wohlfarth ER (ed) Ferromagnetic materials. Vol. 1. North-Holland Publ. Co, Amsterdam, pp 531–589
- Cullen JR, Clark AE (1977) Magnetostriction and structural distortion in rare-earth intermetallics. Phys Rev B 15:4510–4515
- Dhilsha KR, Rama Rao KVS (1993) Investigation of magnetic, magnetomechanical, and electrical properties of the  $\text{Tb}_{0.27}\text{Dy}_{0.73}\text{Fe}_{2-x}\text{Co}_x$  system. J Appl Phys 73:1380–1385
- Feller W (1961) An introduction to probability theory and its applications, 2nd ed. Vol. 1. Wiley, London, pp 175–189
- Fiebig M (2005) Revival of the magnetoelectric effect. J Phys D: Appl Phys 38:R123–R152
- Gicala B, Pszczoła J, Kucharski Z, Suwalski J (1994) Two Slater-Pauling dependences for Dy-3d metal compounds. Phys Lett A 185:491–494
- Gicala B, Pszczoła J, Kucharski Z, Suwalski J (1995) Magnetic hyperfine fields of  $\text{Dy}_x(\text{Fe-Co})_y$  compounds. Solid State Commun 96:511–515
- Gu K, Li J, Ao W, Jian Y, Tang J (2007) The magnetocaloric effect in (Dy,Tb)Co<sub>2</sub> alloys. J Alloys Compd 441:39–42
- Guo ZJ, Zhang ZD, Wang BW, Zhao XG, Geng DY, Li W (2001) Anisotropy compensation and spin reorientation in  $\text{Tb}_{1-x}\text{Dy}_x(\text{Fe}_{0.8}\text{Co}_{0.2})_2$ . J Phys D: Appl Phys 34:884–888
- Ilyushin AS, Nikitin SA, Ngiep NV, Opalenko AA, Tereshina IS, Firov AI (2007) X-ray and Mössbauer studies of the  $\text{Tb}_{0.3}\text{Dy}_{0.7}\text{Fe}_{2-x}\text{Co}_x$  system alloys. Mosc Univ Phys Bull 62:237–239
- Kishore S, Markandeyulu G, Rama Rao KVS, Das TP (1997) <sup>57</sup>Fe Mössbauer investigations on the hydrogenated compounds of  $\text{Dy}_{0.73}\text{Tb}_{0.27}\text{Fe}_{1.5}\text{Co}_{0.5}$ . Solid State Comm 104:735–740
- Laves F (1939) Kristallographie der Legierungen. Naturwissenschaften 27:65–73
- Nan CW, Bichurin MI, Dong S, Viehland D, Srinivasan G (2008) Multiferroic magnetoelectric composites: historical perspective, status, and future directions. J Appl Phys 103:031101
- Nan CW, Liu G, Lin Y (2003) Influence of interfacial bonding on giant magnetoelectric response of multiferroic laminated composites of  $\text{Tb}_{1-x}\text{Dy}_x\text{Fe}_2$  and  $\text{PbZr}_x\text{Ti}_{1-x}\text{O}_3$ . Appl Phys Lett 83:4366–4368
- Politova GA, Tereshina IS, Nikitin SA *et al.* (2005) Effect of hydrogenation on the magnetic and magnetoelastic properties of the  $\text{Tb}_{0.27}\text{Dy}_{0.73}\text{Fe}_2$  and  $\text{Tb}_{0.27}\text{Dy}_{0.73}\text{Co}_2$  compounds with compensated magnetic anisotropy. Phys Solid State 47:1909–1913
- Rietveld HM (1969) A profile refinement method for nuclear and magnetic structures. J Appl Cryst 2:65–71
- Rodriguez-Carvajal J (1993) Recent advances in magnetic structure determination by neutron powder diffraction. Physica B 192:55–69
- Segnan R, Deriu A (1992) Hyperfine fields studies in Laves phase intermetallic compounds. J Magn Magn Mater 104/107:1399–1400
- Senthil Kumar M, Reddy KV, Rama Rao KVS, Das TP (1995) <sup>57</sup>Fe Mössbauer investigations on the  $\text{Dy}_{0.73}\text{Tb}_{0.27}\text{Fe}_{2-x}\text{Ni}_x$  and  $\text{Ho}_{0.85}\text{Tb}_{0.15}\text{Fe}_{2-y}\text{Ni}_y$  systems. Phys Rev B 52:6542–6549
- Stoch P, Onak M, Pańta A, Pszczoła J, Suwalski J (2002) Synthesis and crystal structure of  $\text{Dy}(\text{Fe-Co-Al})_2$ . IEA Monographs. Vol. 5. Instytut Energii Atomowej, Otwock-Świerk (in Polish)
- Stoch P, Pszczoła J, Guzdek P, Chmista J, Pańta A (2005) Electrical resistivity studies of  $\text{Dy}(\text{Fe}_{1-x}\text{Co}_x)_2$  compounds. J Alloys Compd 394:116–121
- Table of periodic properties of the elements (1980) Sargent-Welch Scientific Company, Skokie
- Taylor KNR (1971) Intermetallic rare-earth compounds. Adv Phys 20:551–660
- Wertheim GK (1964) Mössbauer effect: principles and applications. Academic Press, New York, pp 59–71

30. Westwood P, Abell JS, Clarke IH, Pitman KC (1988) Microstructure and magnetostriction in rare-earth-iron alloys. *J Appl Phys* 64:5414–5416
31. Zhang N, Fan J, Rong X, Cao H, Wei J (2007) Magneto-electric effect in laminate composites of  $Tb_{1-x}Dy_xFe_{2-y}$  and Fe-doped  $BaTiO_3$ . *J Appl Phys* 101:063907
32. Zheng X, Zhang P, Fan D, Li F, Hao Y (2005) A structural, magnetostrictive and Mössbauer study of  $Tb_{0.3}Dy_{0.7}(Fe_{0.9}T_{0.1})_{1.95}$  alloys. *Science in China Ser G* 48:750–756